

This article was downloaded by: [Dalian University of Technology]

On: 14 October 2014, At: 01:26

Publisher: Taylor & Francis

Informa Ltd Registered in England and Wales Registered Number: 1072954 Registered office: Mortimer House, 37-41 Mortimer Street, London W1T 3JH, UK



Mechanics Based Design of Structures and Machines: An International Journal

Publication details, including instructions for authors and subscription information:

<http://www.tandfonline.com/loi/lmbd20>

Design Optimization of Connection Section for Concentrated Force Diffusion

Jiaxin Zhang^a, Bo Wang^a, Fei Niu^a & Gengdong Cheng^a

^a State Key Laboratory of Structural Analysis for Industrial Equipment, Department of Engineering Mechanics, Dalian University of Technology, Dalian, Liaoning, China

Accepted author version posted online: 18 Jul 2014. Published online: 25 Sep 2014.

To cite this article: Jiaxin Zhang, Bo Wang, Fei Niu & Gengdong Cheng (2015) Design Optimization of Connection Section for Concentrated Force Diffusion, *Mechanics Based Design of Structures and Machines: An International Journal*, 43:2, 209-231, DOI: [10.1080/15397734.2014.942816](https://doi.org/10.1080/15397734.2014.942816)

To link to this article: <http://dx.doi.org/10.1080/15397734.2014.942816>

PLEASE SCROLL DOWN FOR ARTICLE

Taylor & Francis makes every effort to ensure the accuracy of all the information (the "Content") contained in the publications on our platform. However, Taylor & Francis, our agents, and our licensors make no representations or warranties whatsoever as to the accuracy, completeness, or suitability for any purpose of the Content. Any opinions and views expressed in this publication are the opinions and views of the authors, and are not the views of or endorsed by Taylor & Francis. The accuracy of the Content should not be relied upon and should be independently verified with primary sources of information. Taylor and Francis shall not be liable for any losses, actions, claims, proceedings, demands, costs, expenses, damages, and other liabilities whatsoever or howsoever caused arising directly or indirectly in connection with, in relation to or arising out of the use of the Content.

This article may be used for research, teaching, and private study purposes. Any substantial or systematic reproduction, redistribution, reselling, loan, sub-licensing, systematic supply, or distribution in any form to anyone is expressly forbidden. Terms & Conditions of access and use can be found at <http://www.tandfonline.com/page/terms-and-conditions>

DESIGN OPTIMIZATION OF CONNECTION SECTION FOR CONCENTRATED FORCE DIFFUSION[#]

Jiaxin Zhang, Bo Wang, Fei Niu, and Gengdong Cheng

State Key Laboratory of Structural Analysis for Industrial Equipment,
Department of Engineering Mechanics, Dalian University of Technology,
Dalian, Liaoning, China

In many load carrying thin shell structures, a connection section is arranged to transfer concentrated external forces to its main section. It is very important for the concentrated external forces to diffuse as uniformly as possible. Nevertheless the traditional design of uniform radial rib is not optimized. The present paper studies an integrated optimization procedure for design optimization of connection section. Variance constraint of node forces at the interface between the main section and connection section is firstly proposed as the evaluation criterion of concentrated force diffusion efficiency and introduced into the topology optimization formulation. Afterwards, for improving the manufacturability of the final design the topology optimization results are interpreted and further optimized by size or shape optimization. Two strategies of interpretation are examined. The first strategy is called strategy of making holes, which inserts a number of internal holes of regular geometric features and smooth boundary with B-spline curves in the continuum based on the topology optimization result. In the second strategy, an initial truss-like design is extracted from the characteristic of topology optimization result. Then a further shape and sizing optimization is followed to obtain the final optimal design. An example of design optimization of plane connection section is presented. The effectiveness of the present approach is demonstrated. The respective advantages and disadvantages of the two strategies are discussed.

Keywords: Concentrated force diffusion; Connection section; Design optimization; Integrated optimization.

1. INTRODUCTION

For many load carrying thin shell structures consisting of several sections, such as launch vehicle, it is often needed to design a connection section which transfers the concentrated external force to its main section. For a light and reliable design of the main section, the diffusion efficiency, or the uniformity of the interfacial

Received March 29, 2013; Accepted July 5, 2014

[#]Communicated by Seonho Cho.

Correspondence: Bo Wang, State Key Laboratory of Structural Analysis for Industrial Equipment, Department of Engineering Mechanics, Dalian University of Technology, Dalian, Liaoning, 116023, China; E-mail: wangbo@dlut.edu.cn

Color versions of one or more of the figures in the article can be found online at www.tandfonline.com/lmbd.

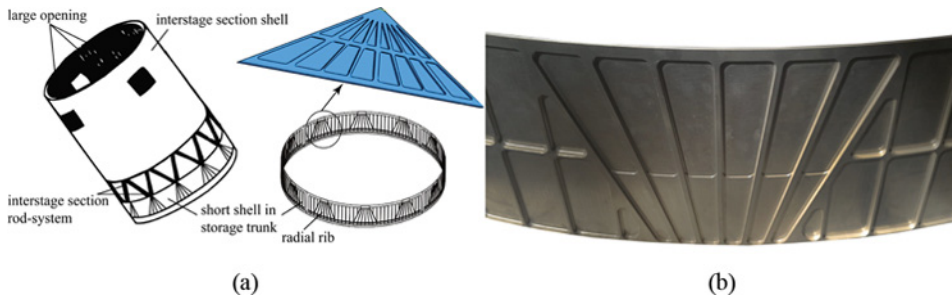


Figure 1 Short shell interstage adapter strengthened with uniform radial ribs: (a) schematic view and (b) detailed design.

force between the connection section and main section is very important. Fig. 1 shows a traditional design of the short cylindrical shell interstage adapter, which is strengthened by a large number of uniform radial ribs in order to diffuse the concentrated force. But the diffusion efficiency of this design is unsatisfactory for its excessively conservativeness and unnecessary weight penalty of the fuel tank design. Thus, it is very important for design optimization of connection section to enhance the diffusion efficiency of concentrated force.

The minimum compliance truss topology design transferring concentrated force on discrete or continuous support has been studied in literatures in the well-known Michell truss layout theory (Rozvany, 1996; Rozvany and Gollub, 1990; Rozvany et al., 1997; Sokół, 2011). Various combinations of line supports and design domains are studied. The relation of concentrated force direction and the line supports is critical to the resulting Michell truss configuration (Lewinski and Rozvany, 2007; Lógó, 2005). The Michell truss layout theory studies the minimum compliance truss topology design of transmitting concentrated force on discrete or continuous support. The relation of concentrated force direction and the line supports is critical to the resulting Michell truss configuration, see Fig. 2(a). When the concentrated force load is perpendicular to the support boundary, optimal Michell truss is a straight-bar. Besides the minimum compliance design of continuum topology optimization would also lead a similar concentrated distribution of material parallel to the load direction, see Fig. 2(b). Nevertheless, differently, the purpose of our study is to mainly discuss how to diffuse the concentrated force by optimizing the transmission path rather than only consider the minimum compliance design.

Topology optimization as a powerful tool has been widely used to obtain a conceptual design in engineering practice (Bendsøe and Sigmund, 2003; Sigmund, 1997). However, the resulting optimum design from topology optimization often needs subsequent detailed post-processing. Otherwise, it is impossible to be applied directly in engineering practice because its material layout includes holes of arbitrary and complex shapes, zigzag boundary, grayscale images and many tiny features, etc (Rozvany, 2001; Sigmund and Petersson, 1998; Yildiz et al., 2003). Most engineering applications require simple geometric feature and smooth boundary, especially for manufacturing.

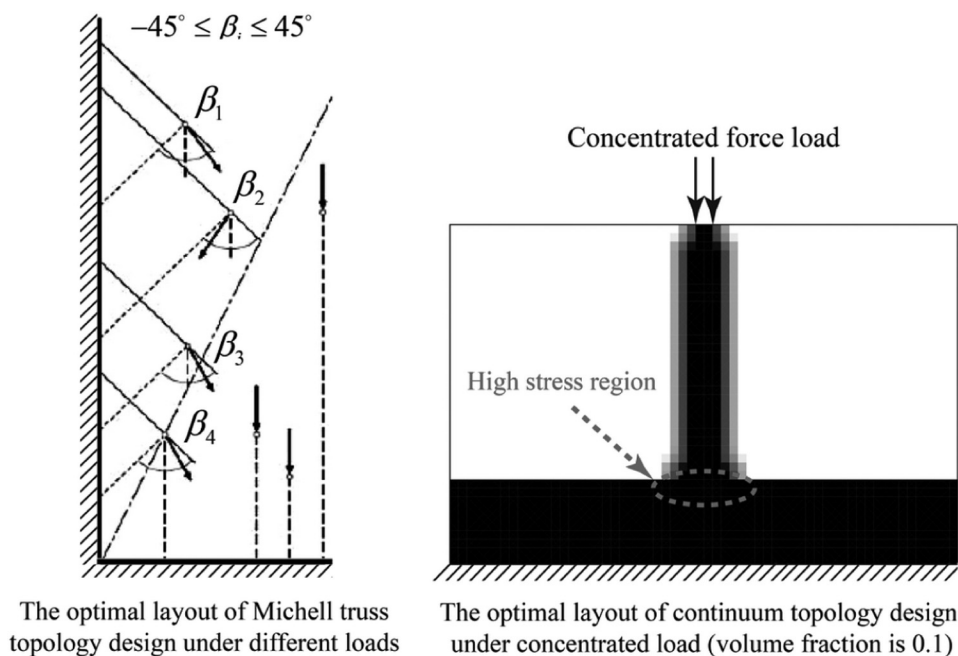


Figure 2 The minimum compliance design of topology optimization.

Such disadvantages of topology optimization can be overcome by properly interpreting the resulting optimum topology followed by shape or size optimization (Bremicker et al., 1991; Sokolowski and Zochowski, 1999; C  a et al., 2000). The first strategy is called strategy of making holes, which inserts a number of internal holes of regular geometric features and smooth boundary with B-spline curves in the continuum based on the topology optimization result. While topology optimization deals with global structural performances such as compliance or natural frequencies, shape optimization controls local performances such as stress by locally adjusting the boundaries of the structure. A critical issue is how to interpret topology optimization result into a representation that can be used in shape optimization (Hsu and Hsu, 2005). Olhoff et al. (1991) proposed a design method to integrate topology and shape optimization. Lin and Chou (1999) proposed an automated image interpretation based on basic geometric shape templates which are used to match holes of various sizes and shapes inside a structure. Hsu et al. (2001) presented a process for integrating topology and shape optimization using density contours. Tang and Chang (2000) approximated the boundaries of the resulting image of topology optimization by using B-spline curves and performed shape optimization by treating control points of the B-spline curves as design parameters.

Krog et al. (2002) proposed a way of interpreting regions with high density of material as structural truss and regions with low density of material as voids, the topology optimized designs can be interpreted as truss-like structures. Truss structure, or frame structure is widely used in civil and mechanical engineering. It is easy to manufacture and its load transmission path is usually very clear which makes maintenance and safety check easy. The beauty of Michell truss theory is

an excellent example. Michell truss illustrates the structure of the optimal force transmission path, which inspired us to adopt truss-like strategy to interpret the resulting conceptual design. Based on truss-like approach it is easy to construct the parameterized optimization model. If the positions of the nodes and the cross sectional areas of the members are optimized, the final optimal truss structures are established (Zhou and Li, 2011). More importantly, in the aerospace, especially rocket, weight reduction is one of the most critical requirements. Compared to the continuum-based shape optimization, truss-like strategy can significantly reduce structural weight through the cross-sectional area and nodal position optimization. Stiffened skin structures have been applied widely in rocket design. Truss-like structure as stiffeners combined with the skin is similar to stiffened skin structure. It is easy for engineers to accept the new design.

In the present paper, we study the integrated design optimization of connection section for concentrated force diffusion. Because of the particularity and importance of the problem, we firstly present the definition of the concentrated diffusion problem. The variance of node forces is introduced as the evaluation criterion of concentrated force diffusion efficiency. In the formulation of topology optimization, minimum compliance objective is subject to constraints on material volume and interfacial nodal force variance. Afterwards, for improving the manufacturability of the final design the topology optimization results are interpreted and further optimized by size or shape optimization. Two strategies of interpretation are examined. The first strategy is called strategy of making holes, which inserts a number of internal holes of regular geometric features and smooth boundary with B-spline curves in the continuum based on the topology optimization result. In the second strategy, an initial truss-like design is extracted from the characteristic of topology optimization result. Then a further shape and sizing optimization is followed to obtain the final optimal design. Optimum designs obtained by distinctive ways of interpretation are compared and discussed.

The organization of the paper is as follows. Section 2 introduces the definition of concentrated force diffusion and presents the conceptual design of concentrated force diffusion. Then, the strategies of making holes and truss-like structures are introduced in Section 3. Numerical examples in Section 4 are used to demonstrate the integrated design procedure by two strategies, and then the respective advantages and disadvantages of the two strategies are discussed in Section 5. Finally, some conclusions are provided in Section 6.

2. CONCENTRATED FORCE DIFFUSION EFFICIENCY AND TOPOLOGY OPTIMIZATION FORMULATION

2.1. Definition of Concentrated Force Diffusion Efficiency

Figure 3(a) shows a structural component schematically. For simplicity, it is only composed of the connection section Ω_1 and the main elastic support section Ω_2 . A concentrated force, or a very large force on a small area, acts on a part of the boundary of Ω_1 . In general, the problem of concentrated force diffusion can be described as design optimization of material distribution in the design domain Ω_1 to transmit the concentrated force \mathbf{F} into a distributed force \mathbf{f} that would be diffused

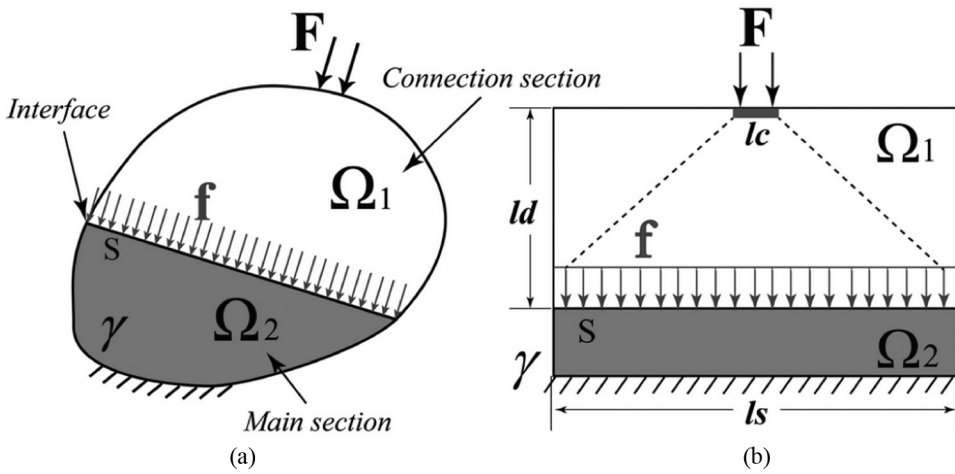


Figure 3 Connection section, main support section and interface.

uniformly at the interface s between Ω_1 and Ω_2 , while keeping the entire structure safety.

It should be emphasized that the concentrated force ideally should act on one single point, but in fact any load should have an action area of finite dimension. Since that, in the present case the concentrated force is defined as distributed force acting on a small area whose dimension is much smaller than the concerned structure. It is assumed that the length scale lc of concentrated force action area is much less than the height ld of connection section, and the height ld of connection section is smaller than the length ls of elastic support section, which means the transmission of concentrated force need to fulfill in a short distance. For the problems discussed below, we have $lc \ll ld$, $ld \approx 0.5ls$, see Fig. 3(b).

Obviously, there would be a high stress region in the action area when lc is small, but many measures such as use of high strength metal material or large local structural thickness can be adopted in engineering practice to avoid material failure in this localized area. Since that, this study mainly concerned that the concentrated force transmitted from the load action area to the main section through the connection section and diffused as uniformly as possible on the interface. Besides, the connection section should not be buckled.

2.2. Topology Optimization Formulation

In order to diffuse the concentrated force as uniformly as possible, the traditional topology optimization formulation of minimum compliance has been modified by introducing the uniform stress constraint at the interface. Continuum topology optimization with stress constraints has been extensively studied, but there are still many difficulties to be overcome (Bendsøe and Sigmund, 2003; Cheng and Guo, 1997; Cheng and Jiang, 1992; Duysinx and Bendsøe, 1998). To avoid the difficulty, in the present study the uniformity of nodal forces at the interface instead of stress, is selected as the criterion to evaluate the diffusion efficiency

of concentrated force. The structural component in Figure 3 is discretized by a unified finite element mesh. For convenience of the further derivation, the interface s coincides with the mesh line. The stiffness matrix \mathbf{K} of the entire structure is the sum of the two parts:

$$\mathbf{K} = \mathbf{K}_1 + \mathbf{K}_2. \quad (1)$$

where \mathbf{K}_1 and \mathbf{K}_2 are the stiffness matrices of the connection and main support sections, and the dimension of \mathbf{K}_1 and \mathbf{K}_2 is expanded to be the same of \mathbf{K} . The governing equation of the entire structure is

$$\mathbf{K}\mathbf{u} = \mathbf{F}. \quad (2)$$

where \mathbf{u} consists of nodal displacement \mathbf{u}_1 and \mathbf{u}_2 in the domain Ω_1 and Ω_2 , respectively.

Let us consider M nodes at the interface and denote f_j the interfacial vertical nodal force through the investigative nodes in the j -th degrees of freedom,

$$f_j = \delta_j^T \mathbf{K}_2 \mathbf{u} \delta_j = \{0, 0, \dots, 1, \dots, 0\}^T \quad (3)$$

The unit 1 appears at the j -th position in the vector δ_j . The variance C_1 of nodal forces describes the uniformity of the interfacial forces, or the diffusion efficiency of concentrated force,

$$C_1 = \sum_{j=1}^M (f_j - \bar{f})^2 / M \quad (4)$$

where M represents the investigative node number at the interface S , $\bar{f} = \sum_{j=1}^M f_j / M$ is the mean value of the nodal forces on the investigative nodes.

Now let us formulate the topology optimization problem of connection section with constraint on concentrated force diffusion efficiency. With SIMP method, material density in each element of the connection section is chosen as design variable. Minimum structural compliance is taken as the objective function subject to constraints on the structural volume and the upper bound of the variance of interfacial nodal forces. Its mathematical formulation can be stated as

$$\begin{aligned} \text{find : } & \boldsymbol{\rho} = \{\rho_1, \rho_2, \dots, \rho_N\}^T \\ \text{min : } & Obj = \mathbf{u}^T \mathbf{K} \mathbf{u} \\ \text{s.t. : } & C_1 = \sum_{j=1}^M (f_j - \bar{f})^2 / M \leq C^* \\ & : C_2 = \sum_{e=1}^N \rho_e v_e \leq V^* \\ & : 0 < \rho_{\min} \leq \rho_e \leq 1, \quad e = 1, 2, \dots, N \end{aligned} \quad (5)$$

where the structural compliance $\mathbf{u}^T \mathbf{K} \mathbf{u}$ is the objective function, ρ_e and v_e is the e -th element density and area, respectively, V^* is the maximum allowable material

volume. The upper bound C^* of variance constraint reflects the desired diffusion efficiency of concentrated force. Smaller C^* means higher diffusion efficiency.

2.3. Sensitivity Analysis

The sensitivity of structural compliance and volume constraint are

$$\frac{\partial Obj}{\partial \rho_e} = -\mathbf{u}_e^T \frac{\partial \mathbf{k}_e}{\partial \rho_e} \mathbf{u}_e, \quad \frac{\partial C_2}{\partial \rho_e} = v_e. \quad (6)$$

where the subscript e represents the e -th element in the design domain.

The sensitivity of nodal force is derived by using the adjoint method as:

$$\begin{aligned} \frac{\partial f_j}{\partial \rho_e} &= \frac{\partial(\delta_j^T \mathbf{K}_2 \mathbf{u})}{\partial \rho_e} - \lambda^T \frac{\partial(\mathbf{K} \mathbf{u} - \mathbf{f})}{\partial \rho_e} \\ &= \frac{\partial(\delta_j^T \mathbf{K}_2)}{\partial \rho_e} \mathbf{u} + \delta_j^T \mathbf{K}_2 \frac{\partial \mathbf{u}}{\partial \rho_e} - \lambda^T \left(\frac{\partial \mathbf{K}}{\partial \rho_e} \mathbf{u} + \mathbf{K} \frac{\partial \mathbf{u}}{\partial \rho_e} \right) \\ &= \frac{\partial(\delta_j^T \mathbf{K}_2)}{\partial \rho_e} \mathbf{u} - \lambda^T \frac{\partial \mathbf{K}}{\partial \rho_e} \mathbf{u} + (\delta_j^T \mathbf{K}_2 - \lambda^T \mathbf{K}) \frac{\partial \mathbf{u}}{\partial \rho_e} \\ &= \frac{\partial(\delta_j^T \mathbf{K}_2)}{\partial \rho_e} \mathbf{u} - \lambda^T \frac{\partial \mathbf{K}}{\partial \rho_e} \mathbf{u} \end{aligned} \quad (7)$$

where the adjoint vector λ is solved by the adjoint equation

$$\mathbf{K} \lambda = \mathbf{K}_2 \delta_j \quad (8)$$

Thus, the sensitivity of the variance constraint of nodal forces is derived as follows:

$$\frac{\partial C_1}{\partial \rho_i} = \frac{2}{M} \sum_{j=1}^M (f_j - \bar{f}) \left(\frac{\partial f_j}{\partial \rho_i} - \frac{\partial \bar{f}}{\partial \rho_i} \right), \quad \frac{\partial \bar{f}}{\partial \rho_e} = \frac{1}{M} \sum_{j=1}^M \frac{\partial f_j}{\partial \rho_e}. \quad (9)$$

where $\partial \bar{f} / \partial \rho_e$ is the sensitivity of the mean value of the nodal forces.

With the sensitivity available, the optimization formulation (5) is solved using MMA optimizer (Svanberg, 1987). Linear density filter strategy is applied during the iteration in order to avoid numerical instabilities.

2.4. Investigation of Influence of C^*

This simple example is to verify the effect of variance constraint through comparison of different C^* . Figure 4 shows the geometry and boundary conditions of a plane structure. The mid-point of the upper side is subject to a vertical concentrated force $F = 100 \text{ N}$. The allowable volume fraction is 30%, Young's modulus is 70 MPa and Poisson's ratio is 0.3. The entire domain is meshed into 2400 four-node plane stress elements (60×40). The connection section is the design domain. The main section is non-design domain. All of the 61 nodes at the interface between the two sections are selected as the investigative nodes.

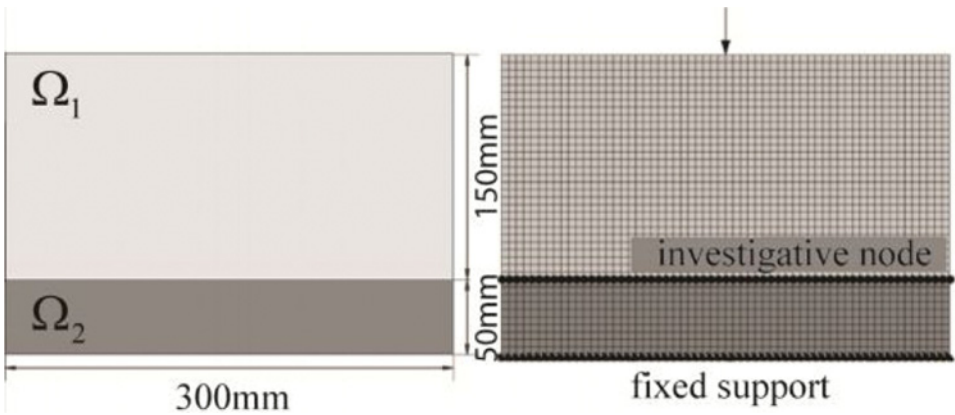


Figure 4 Geometrical model and boundary conditions for numerical example.

Table 1 lists the optimal results as well as the objective function values under different upper bound of variance constraint for $C^* = 0.01, 0.1, 1, \infty$, and it can be seen that as the allowed variance C^* increases, the objective function value gradually decreases and the nodal forces deviate more from its mean value. In other words, the concentrated force diffusion efficiency decreases and the structural stiffness gradually increases as the material distribution is more and more concentrated in the middle of the design domain. A proper balance between structural stiffness and diffusion efficiency is very important.

3. TWO STRATEGIES OF INTERPRETATION

It can be seen that the topology optimization results in Table 1 have the following characteristics: (1) material zigzag boundary, (2) gray-scale intermediate regions, (3) small local structural features. Because of these characteristics, it is not easy to directly apply topology optimization results in detailed design such as shape or sizing optimization. Therefore, two strategies of interpretation of topology optimization results are examined.

3.1. Making Holes Strategy

The first strategy is called strategy of making holes, which inserts a number of internal holes of regular geometric features and smooth boundary with B-spline curves in the continuum according to the topology optimization result.

Table 1 Topology optimization results under different variance constraints

C^*	0.01	0.1	1.0	Infinite
Object (N)	67.0052	61.5713	46.9441	39.7281
Optimum topology				

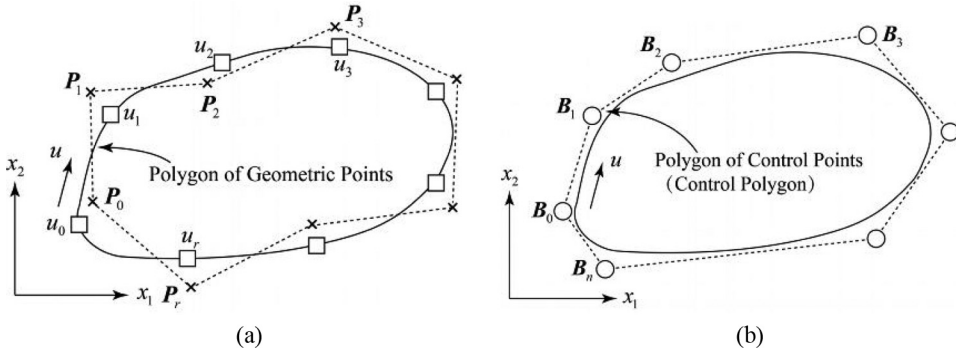


Figure 5 B-spline curve fitting: (a) Curve fitting for geometric points \mathbf{P}_j and (b) B-spline curve with control points \mathbf{B}_j .

3.1.1. Boundary smooth and approximation using B-spline curves.

After topology optimization, the boundaries of the optimized image are parameterized by using B-spline curves. To reduce boundary wiggles inherited from the finite element mesh, smoothing procedure is performed before boundary approximation (Tang and Chang, 2000). New smoothed boundary points are obtained by applying a simple averaging filter to the boundary FEM nodes:

$$\mathbf{P}_j = \frac{1}{5}(\mathbf{P}'_{j-2} + \mathbf{P}'_{j-1} + \mathbf{P}'_j + \mathbf{P}'_{j+1} + \mathbf{P}'_{j+2}), \quad j = 2, \dots, r-2. \quad (10)$$

where \mathbf{P}_j is the position vector of the j -th point in the new smoothed boundary, \mathbf{P}'_j is the position vector of the j -th point in the FEM boundary of the topology optimization results. $r+1$ is the total number of geometric points in the concerned boundary. This averaging process reduces the wiggle property of the boundary inherited from the finite element mesh.

Using the least square fitting for geometric points on the new smoothed boundary, the best approximate boundaries with B-spline curves are obtained by minimizing the distance sum g between the curve $\mathbf{x}(u)$ and the points \mathbf{P}_j . The distance sum g is defined as

$$g = \sum_{j=0}^r |\mathbf{P}_j - \mathbf{x}(u_j)|^2 \quad (11)$$

where $\mathbf{x}(u)$ is the fitting B-spline curve, u is the parametric coordinate of the curve, $\mathbf{x}(u_j) = [x_1(u_j), x_2(u_j), x_3(u_j)]$ is the position vector of the fitting B-spline curve at u_j , and u_j is defined by the length ratio of the polygon formed by the geometric points \mathbf{P}_j , as illustrated in Fig. 5(a). The values of u_j are determined by

$$u_0 = 0 \quad \text{and} \quad u_j = u_{j-1} + \frac{|\mathbf{P}_j - \mathbf{P}_{j-1}|}{d}, \quad j = 1, 2, \dots, r. \quad (12a)$$

$$d = \sum_{j=1}^r |\mathbf{P}_j - \mathbf{P}_{j-1}|. \quad (12b)$$

Note that u_j can be further adjusted for reducing the curve fitting error using, for example, the chord length parameterization method (Tang, 1999). Mathematically, the B-spline curve is defined as (Mortenson, 1985),

$$\mathbf{x}(u) = \sum_{i=0}^n \mathbf{B}_i N_{i,k}(u), \quad (0 \leq u \leq 1) \quad (13)$$

where \mathbf{B}_i is the i -th control point shown in Fig. 5(b), $n+1$ is the number of control points, and $N_{i,k}(u)$ is the basis function of the B-spline curve defined recursively as

$$N_{i,k}(u) = \frac{(u - t_i)N_{i,k-1}(u)}{t_{i+k-1} - t_i} + \frac{(t_{i+k} - u)N_{i+1,k-1}(u)}{t_{i+k} - t_{i+1}} \quad (14a)$$

$$N_{i,1}(u) = \begin{cases} 1 & t_i \leq u \leq t_{i+1} \\ 0 & \text{otherwise} \end{cases} \quad (14b)$$

where $[t_i, t_{i+1})$ is a knot span formed by the two consecutive knots t_i and t_{i+1} , and $k-1$ is the polynomial order of the basis functions. In order to minimize g , the derivative of g with respect to the $n+1$ control points is set to zero. For simplicity, considering only the ℓ -th control point, one has

$$\frac{dg}{d\mathbf{B}_\ell} = \sum_{j=0}^r \left| -2\mathbf{P}_j \sum_{i=0}^n N_{i,k}(u_j) + 2 \sum_{i=0}^n N_{i,k}(u_j) \left(\sum_{i=0}^n N_{i,k}(u_j) \mathbf{B}_\ell \right) \right| = 0 \quad (15)$$

For $\ell = 0, \dots, n$, the above expression can be rewritten in a matrix form as

$$\mathbf{N}^T \mathbf{N} \mathbf{B} = \mathbf{N}^T \mathbf{P} \quad (16)$$

where $\mathbf{B} \in \mathbf{R}^{(n+1) \times 3}$ and $\mathbf{P} \in \mathbf{R}^{(r+1) \times 3}$ denote the vectors of control points and smoothed boundary points, respectively, and the matrix $\mathbf{N} \in \mathbf{R}^{(r+1) \times (n+1)}$ is defined as

$$\mathbf{N} = \begin{bmatrix} N_{0,k}(u_0) & N_{1,k}(u_0) & \cdots & N_{n,k}(u_0) \\ N_{0,k}(u_1) & N_{1,k}(u_1) & \cdots & N_{n,k}(u_1) \\ \vdots & \vdots & \ddots & \vdots \\ N_{0,k}(u_r) & N_{1,k}(u_r) & \cdots & N_{n,k}(u_r) \end{bmatrix}_{(r+1) \times (n+1)} \quad (17)$$

Some of the control points obtained from Eq. (16) will be selected as design variables for shape optimization.

3.1.2. Shape and sizing optimization. After a number of holes of smooth boundary with B-spline curves are set in the continuum, we obtain a new design. The commercial software ABAQUS is employed to set up a parametric model and analyze its performance. The structural volume constraint might be not satisfied since the shape has been modified in the interpretation process. Thus, for shape optimization, we would consider the structural volume as the design constraint,

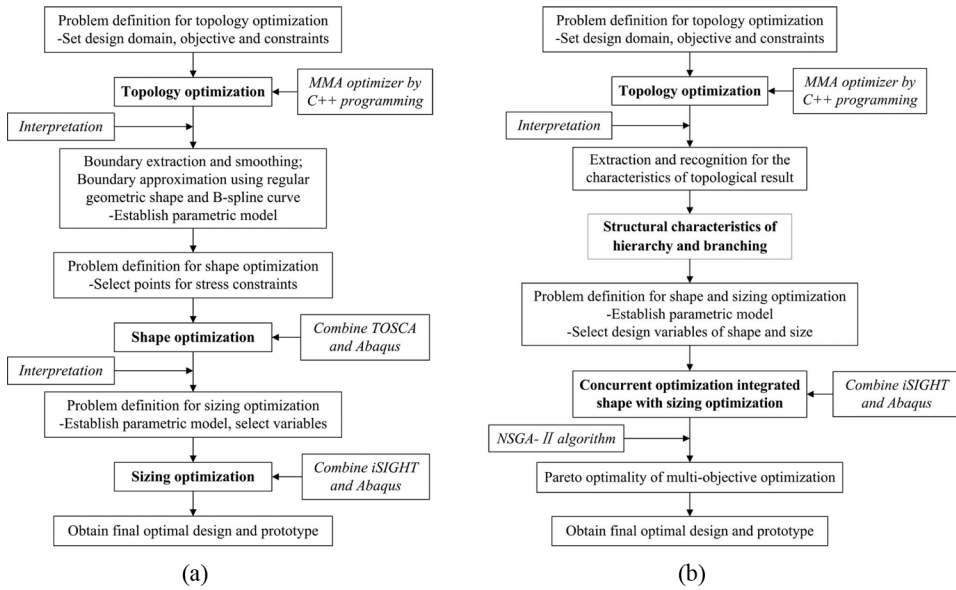


Figure 6 The flowchart of two interpretation strategies: (a) Making holes and (b) Truss-like.

and the objective function is to decrease the local high stress which is not considered in topology optimization. A further detailed design is performed by sizing optimization. The objective function is to improve the diffusion efficiency subjected to the constraints on the structural strength, volume, and stability. The flow chart of the optimization process is shown in Fig. 6(a).

3.2. Truss-Like Strategy

For the truss-like strategy, we should firstly recognize and extract the characteristics of topology optimization result according to its high density contour. For the present concentrated force diffusion problem with low allowable volume fraction, the continuum enclosed by high density contour is a truss-like structure. The positions of the nodes and the cross sectional areas of the members should be interactively determined. Some of the nodal positions and cross-sectional areas are considered as design variables. In this way, a parametric model based on the truss-like feature would be established. Furthermore, the positions of the nodes and the cross sectional areas of the members are optimized and final topological optimal structures are obtained. The advantages of truss-like strategy may be the much lower volume than making holes strategy, but it is very difficult for us to provide an accurate and suitable volume constraint. Furthermore, in order to balance volume reduction and diffusion efficiency, a multi-objective optimization algorithm based on non-dominated sorting genetic algorithm (NSGA-II) is introduced (Deb et al., 2002), and then used to find a detailed design meeting strength and stability requirement. The optimization process is illustrated by the flowchart, as shown in Fig. 6(b).

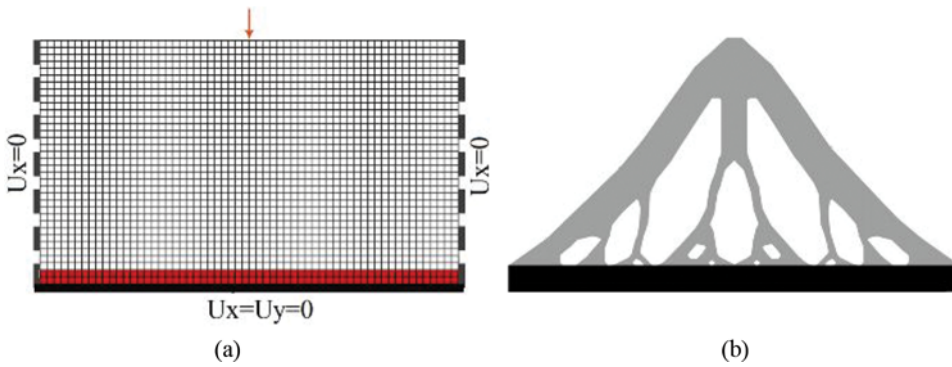


Figure 7 Topology optimization and feature extraction: (a) Initial finite element model and (b) Optimal topological result.

4. NUMERICAL EXAMPLE

The following example shows the integrated design optimization approach and presents an optimum design of a plane connection section. The design domain of the connection section is a $600\text{ mm} \times 330\text{ mm}$ rectangle, the main section is a non-design domain of $600\text{ mm} \times 20\text{ mm}$ rectangle, and the thickness is 20 mm . The nodal displacement at its left and right side is subject to symmetry constraints ($U_X = 0$, $ROT_Y = 0$, $ROT_Z = 0$), the lower side is fixed, and the upper side is subject to a downward local uniform force of 120 MPa and zero normal displacement ($U_Z = 0$). The material is aluminum alloy. Young's modulus is 70 GPa , Poisson's ratio is 0.3 , Yield stress is 280 MPa and density is $2.8 \times 10^3\text{ kg/m}^3$. The requirements of structural design includes: (1) the volume of the connection section structure does not exceed 30% of the design domain; (2) the maximum stress in the Y direction at the interface is minimized; (3) the structure does not fail for any forms of instability; (4) the design is simple and reasonable which meets the requirements of manufacturability. In order to satisfy these above requirements, minimum compliance topology optimization with concentrated force diffusion efficiency as conceptual design would be carried out in the first phase and then an integrated design optimization approach would be applied.

4.1. Topology Optimization

The optimization model can be simplified as a plane stress model in topology optimization phase, as shown in Fig. 7(a). 60×35 four-node plane stress elements of 10 mm are applied to mesh the structural domain. All nodes at the interface are selected as the investigative nodes, and the variance constraint C^* of vertical nodal interfacial forces is equal to 0.01 . Figure 7(b) shows the optimal topological result. The irregular geometry makes it very difficult for parametric model description. But the extracted structural configuration provides a basis for further interpretation of optimized topological result.

We can use two strategies to implement a further extraction on a basis of the result shown in Fig. 7(b). The first strategy is called making holes which

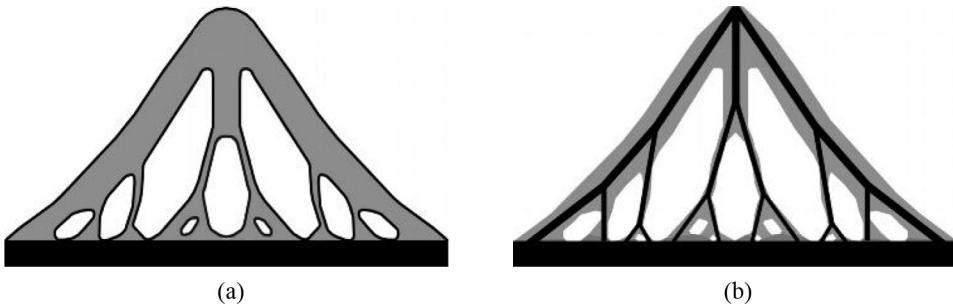


Figure 8 Topology feature extraction: (a) Making holes strategy and (b) Truss-like strategy.

derived from the intuitive understanding of optimized topology result, as shown in Fig. 8(a). The second strategy is called truss-like which is inspired from the optimal topological layout of Michell truss, as shown in Fig. 8(b).

4.2. Making Holes Strategy

4.2.1. Interpretation of characteristics. The strategy of making holes is based on matching the arbitrary shape holes inside the optimum topology with predefined simple geometric features and approximating its external boundary with B-spline curves, as illustrated in Fig. 9(a). In order to avoid the local high stress in the sharp corners, some chamfers are introduced appropriately. Figure 9(b) shows the geometric model. Its two symmetric external boundaries are approximated by using two separate fourth orders of B-spline curves with five control points, which can be calculated automatically by Python script in Abaqus.

After the aforementioned step, a parametric geometric model is built. In order to facilitate further consideration of out of plane buckling constraint, the parametric model is meshed by 8-node hexahedral body solid elements C3D8R of 4mm and analyzed by three dimensional FEM. The maximum stress in the Y direction at the investigative nodes, which relates to the diffusion efficiency of concentrated force, is 77.22 MPa. The structural volume is $1.2294 \times 10^{-3} \text{ m}^3$ which accounts for 31.05%

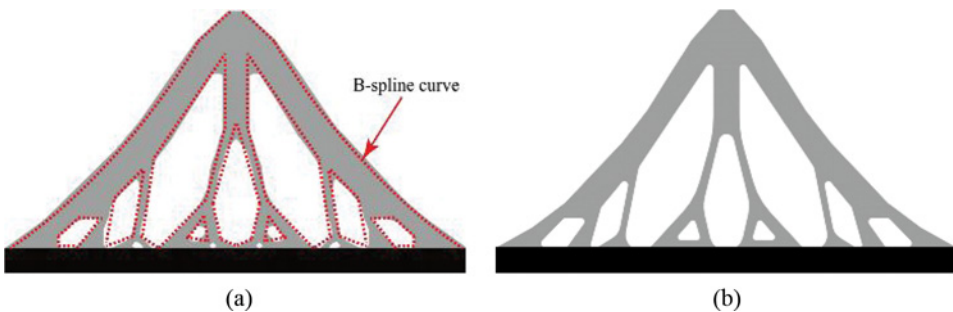


Figure 9 (a) Interpretation using simple geometric features and B-spline curves and (b) Parametric geometry model after interpretation.

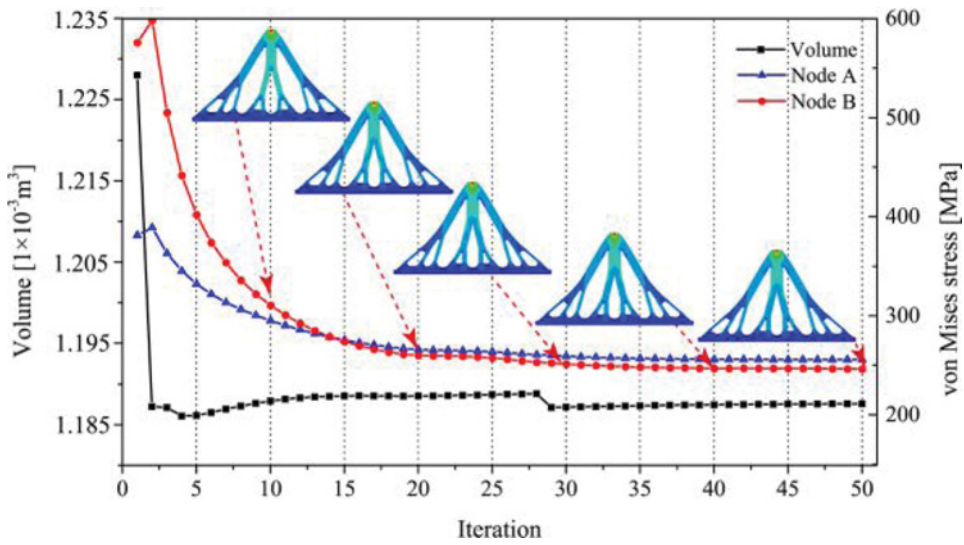


Figure 10 Iteration history of shape optimization.

of the design domain and slightly violates the volume constraint. Buckling analysis using Lanczos linear eigenvalue method focus on the global stability of the structure, and the buckling load factor is 1.7023 that means instability does not occur in the given load conditions. The maximum von Mises stress in the action area of concentrated force is very high which is expected because the concentrated force load acts on a very small area. However, in engineering practice, several effective measures can be used to solve it. For example, higher strength material and large thickness can be arranged in the load action area. We focus on the stress of overall structure rather than the action area of concentrated force, but there are still some regions that exceed 280 MPa after topology optimization. Thus, a further shape optimization is highly necessary.

4.2.2. Shape optimization. Since the parametrical model does not satisfy the constraints on material volume and maximum stress, shape optimization is further applied. The shape optimization is implemented by integrated TOSCA with Abaqus. The free boundary nodes of structure are chosen as the design variables. Minimizing the maximum von Mises stress is taken as the objective function subject to constraints on the structural volume in shape optimization. The Node A and B are selected as two special observation nodes because of their higher stress after topology optimization.

Figure 10 shows the iteration history of shape optimization. It is so difficult to decrease the maximum von Mises stress of overall structure since that the stress in the action area is always very high. Thus we concern more about the two selected nodes. After 50 iterations, the von Mises stress of Node A and B decrease significantly from initial 575.5 MPa and 381.1 MPa to 246.1 MPa and 255.8 MPa, respectively. The structural volume also decreases from initial $1.2294 \times 10^{-3} \text{ m}^3$ to $1.1875 \times 10^{-3} \text{ m}^3$. It can be seen from the iteration history that the structural volume

decreases fast and the maximum von Mises stress increases slightly in the early iteration. In the later iterations, the structural volume remains nearly constant and the maximum von Mises stress gradually decreases with the continuous adjustment of the structural shape.

The performance of optimum design after shape optimization is that the maximum stress in the Y direction at the interface is 93.23 MPa, which is much higher than the initial parametric model before shape optimization. This is because the material distribution near the main support section is very sensitive to the diffusion efficiency. There are some local high stress regions caused by the non-uniform reduction of materials near the main support section. The von Mises stress of overall structure meets the design requirements except for the concentrated force action area.

4.2.3. Sizing optimization. Based on mechanical intuition, five design variables are identified in the sizing optimization as shown in Fig. 11. The material distribution near the interface is determined by d_1 , d_2 , d_3 , d_4 , and d_5 . The diffusion efficiency should be much better when the value of d_1 , d_2 , d_3 , d_4 , and d_5 is high, but it might violate the volume constraint.

In sizing optimization, the objective function is to minimize the stress in the Y direction at the investigative nodes subject to the constraints on the structural strength, volume and stability. The mathematical formulation of this sizing optimization problem can be stated as

$$\begin{aligned}
 &\text{find : } \mathbf{X} = \{d_1, d_2, d_3, d_4, d_5\}^T \\
 &\text{min : } Obj = \max(\sigma_Y) \\
 &\text{s.t. : } C_1 = \max(\sigma_{mises}) \leq 280 \\
 &\quad : C_2 = \text{volume} \leq 1.1875 \\
 &\quad : C_3 = \lambda_1 > 1 \\
 &\quad : \mathbf{X}_{\min} \leq \mathbf{X} \leq \mathbf{X}_{\max}
 \end{aligned} \tag{18}$$

where $\max(\sigma_Y)$ represents the maximum stress in the Y direction, C_1 , C_2 , and C_3 are constraints on the structural strength, volume, and the global buckling load factor.

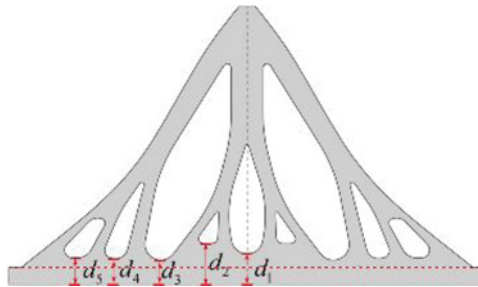


Figure 11 Design variable of sizing optimization.

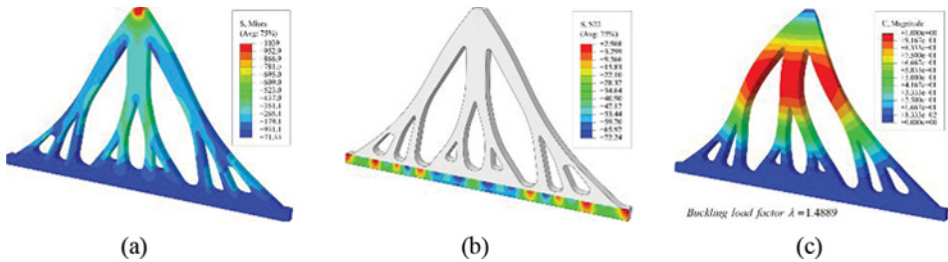


Figure 12 Performance of optimum design after sizing optimization: (a) von Mises stress, (b) Stress in the Y direction and (c) Buckling mode.

X_{\min} and X_{\max} are the lower and upper bound of design variables, respectively. The stress constraint in the action area is not considered.





Sizing optimization is realized by iSIGHT combined with ABAQUS software. Multi-island genetic algorithm (MGA) as one kind of genetic algorithm, which has been widely used for solving global optimization problems, is applied. The initial values, upper and lower bound are equal to 35 mm, 50 mm, and 20 mm, respectively, and the optimal value of the five design variables d_1 , d_2 , d_3 , d_4 , d_5 are equal to 37.18 mm, 48.25 mm, 26.19 mm, 27.37 mm, 32.15 mm, respectively. After the sizing optimization, the maximum stress in the Y direction is 72.24 MPa which has a very significant improvement compared to the result of shape optimization, and the von Mises stress and buckling mode of the overall structure both satisfy the design requirement, as shown in Fig. 12.

The results of optimal designs in the three steps are shown in Table 2. A significant improvement in diffusion efficiency can be viewed with the integrated process from conceptual to detailed design.

4.3. Truss-Like Strategy

4.3.1. Truss configuration extraction. In the following, we apply the truss-like strategy to post-process the optimum topological result in Fig. 7(b).

Table 2 Optimal designs at three stages of design process and the final CAD model

Design process	Topology optimization	Shape optimization	Sizing optimization	CAD model
Geometry				
Maximum stress in the Y direction	77.22 MPa	93.23 MPa	72.24 MPa	72.69 MPa
Structural volume ($< 1.1875 \times 10^{-3} \text{ m}^3$)	$1.2294 \times 10^{-3} \text{ m}^3$	$1.1875 \times 10^{-3} \text{ m}^3$	$1.1875 \times 10^{-3} \text{ m}^3$	$1.1877 \times 10^{-3} \text{ m}^3$
First-order buckling load factor	1.7023	1.6890	1.4889	1.4828

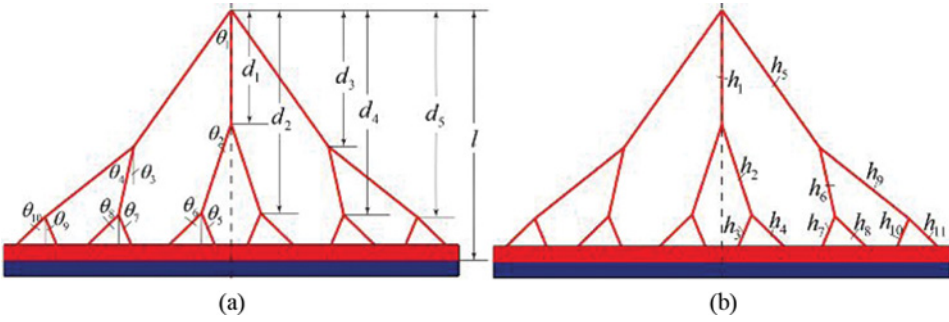


Figure 13 (a) Shape parameters and (b) Size parameters.

Figure 7(b) shows the extraction results which are used to eliminate the gray areas and some small features. Taking into account this configuration, a truss-like structure of Fig. 8(b) can be established. The resulting truss-like structure shows a characteristic of branching and hierarchy. As shown in the paper of Waller (2006), that branching structures mimic trees and have a high strength-to-volume ratio for supporting compressive loads. Liu et al. (2008) and Yan et al. (2008) both also demonstrate the superiority of truss-like structure.

4.3.2. Integrated shape and sizing optimization. Our proposed approach is to establish a concurrent method integrated shape with sizing optimization. The lengths (d_1, d_2, d_3, d_4) and angles ($\theta_i, i = 1, 2, \dots, 10$) of branches as shape parameters determine the distribution of members, while the cross sectional areas are taken as size parameters, including width parameters h_i ($i = 1, 2, \dots, 10$) and height parameters t_i ($i = 1, 2, \dots, 10$), as shown in Fig. 13.

The truss member is modeled by a two-node linear beam element (B21), and the elastic non-design domain by the four-node bilinear plane stress quadrilateral element (CPS4R). The two types of different element join together at the interface between the connection section and the main section. We mainly concentrate on the element stress at the interface between the red region and blue region. This modeling approach causes very high stress between truss member and the main support section structure. In this phase, we mainly focus on the concentrated force diffusion efficiency, and structural volume while taking into account the stability requirement. The high local stress at the connection between two different type elements is not considered at this stage. Thus, a multi-objective optimization model is used to achieve optimal diffusion efficiency with a minimum volume. The formulation takes the following form

$$\begin{aligned}
 &\text{find : } \mathbf{X} = \{\mathbf{d}^T, \boldsymbol{\theta}^T, \mathbf{h}^T\}^T \\
 &\text{min : } Obj_1 = Volume(\mathbf{X}) \\
 &\quad : Obj_2 = Maximum\ stress\ Y(\mathbf{X}) \\
 &\text{s.t. : } C_1 = Max(\sigma_v) \leq \bar{C} \\
 &\quad : C_2 = \lambda_1 > 1.0 \\
 &\quad : \mathbf{X}_{min} \leq \mathbf{X} \leq \mathbf{X}_{max}
 \end{aligned} \tag{19}$$

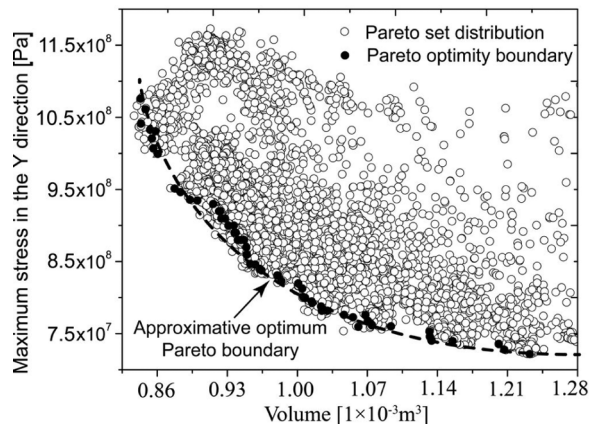


Figure 14 Multi-objective optimization results.

where \mathbf{X} is a set of design variables including the shape and size parameters in Table 4, the objective function Volume (\mathbf{X}) is the structural volume, and Maximum stress $Y(\mathbf{X})$ refers the maximum stress in the Y direction. $Max(\sigma_v)$ is the maximum von Mises stress as strength constraint and λ_1 is the first order buckling load factor as stability constraint. \mathbf{X}_{min} and \mathbf{X}_{max} are the lower and upper bound of design variables, respectively. The multi-objective optimization algorithm based on non-dominated sorting genetic algorithm (NSGA-II) is employed to solve this optimization problem.

4.3.3. Optimum result. The Pareto optimum solutions of multi-objective optimization in Eq. (19) are shown in Fig. 14, in which the ordinate is the objective maximum stress in the Y -direction and the abscissa is the material volume. The Pareto optimality boundary (black points in Fig. 14) is an approximately parabolic shape which demonstrates a certain competitive relationship between maximum stress and volume.

According to actual engineering requirement, designer can select an optimal point on the Pareto optimality boundary. In this study, we choose the optimal point of diffusion efficiency as the optimal design, thus the maximum stress in the Y direction at the interface is 73.44 MPa, and structural volume is $0.9969 \times 10^{-3} \text{ m}^3$. The first order load factor of buckling is 1.4974, which meets the stability requirement. The geometry of optimal design shows the characteristics of three levels hierarchy and branching structure. Both sides of branching structure are stronger that they can transmit the concentrated force into both sides of the main support section much more uniformly. The bifurcations near the main support section are relatively thinner in order to avoid the high level of stress, as shown in Fig. 15(a). The performance of optimal design is shown in Fig. 15(b) and (c). The upper and lower bound, initial and optimal value of design variables in shape and size optimization are given in Tables 3 and 4.

A detailed distribution of stress in the Y direction is shown in Fig. 15(a). The maximum value of stress is 73.44 MPa and more than 70% of the investigated elements have stress between 30 and 70 MPa. For the distribution of von Mises

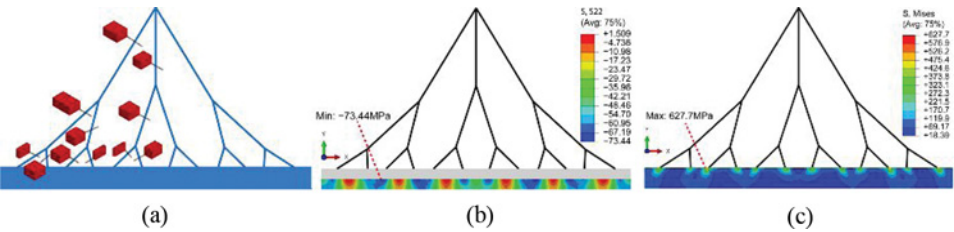


Figure 15 Optimal design: (a) Geometry, (b) Stress distribution in the Y direction and (c) von Mises stress.

stress, some points of high stress appear at the interface between two-node linear beam element and four-node bilinear plane stress element. But the high stress does not present in the whole region of main support section. Some local measures can be taken to decrease and eliminate the high level stress caused by different elements of connection.

5. COMPARISON AND DISCUSSION

Two strategies of making holes and truss-like both have their own advantages and disadvantages. The comparison of objective function value and constraints between the two strategies is shown in Table 5 and Fig. 16.

The strategy of making holes as the traditional method is usually used to solve the interpreted connection from the conceptual design to detailed design. More than 70% of the investigated element of the stress in the Y direction is between 30 and 70 MPa and no obvious high level stress exists. The advantages of the strategy include a more precise identification and interpretation of the result from topology optimization. However, it is so difficult to accomplish automatic identification and interpretation for the whole process without the human design

Table 3 Design variables of shape parameters

Shape parameters	$d_1/$ mm	$d_2/$ mm	$d_3/$ mm	$d_4/$ mm	$d_5/$ mm	$\theta_1/$ rad	$\theta_2/$ rad	$\theta_3/$ rad	$\theta_4/$ rad	$\theta_5/$ rad	$\theta_6/$ rad	$\theta_7/$ rad	$\theta_8/$ rad	$\theta_9/$ rad	$\theta_{10}/$ rad
Upper bound	350	350	350	350	350	0.1	0.1	0.1	0.1	0.1	0.1	0.1	0.1	0.1	0.1
Lower bound	100	100	100	100	100	1.0	1.0	1.0	1.0	1.0	1.0	1.0	1.0	1.0	1.0
Initial value	200	200	200	300	300	0.5	0.4	0.4	0.4	0.6	0.4	0.6	0.4	0.6	0.6
Optimal value	152	268	181	270	273	0.55	0.32	0.30	0.28	0.29	0.81	0.27	0.80	0.05	1.0

Table 4 Design variables of size parameters

Size parameters	$h_1/$ mm	$h_2/$ mm	$h_3/$ mm	$h_4/$ mm	$h_5/$ mm	$h_6/$ mm	$h_7/$ mm	$h_8/$ mm	$h_9/$ mm	$h_{10}/$ mm	$h_{11}/$ mm
Upper bound	40.0	40.0	40.0	40.0	40.0	40.0	40.0	40.0	40.0	40.0	40.0
Lower bound	4.0	4.0	4.0	4.0	4.0	4.0	4.0	4.0	4.0	4.0	4.0
Initial value	15	15	15	15	15	15	15	15	15	15	15
Optimal value	15.38	19.35	14.08	4.91	25.49	17.17	4.50	17.19	31.71	20.01	6.36

Table 5 Comparison of two different strategies

Strategy	Maximum stress (in the Y direction)	Structural volume	Buckling load factor
Making holes	72.24 MPa	$1.1875 \times 10^{-3} \text{ m}^3$	1.4889
Truss-like	73.44 MPa	$0.9969 \times 10^{-3} \text{ m}^3$	1.4974

experience. For complex boundaries or multi-holes model or three-dimensional solid, the optimization process is much more convoluted and time-consuming.

The strategy of truss-like presents an essential and excellent force transferring path by the extraction and recognition of the characteristics without considering the gray-scale elements and rough boundary problems occurring in topology optimization. Then through the shape and sizing optimization, truss-like strategy can obtain a much clearer and easier design using a lower volume cost but the diffusion efficiency seems as good as the strategy of making holes. The maximum stress in the Y direction is only 1.7% higher than the strategy of making holes, but the structural volume has a significant reduction by 16.1%. However, there are still some severe limitations. The local high stress at the interface between different element types is far higher as well as mesh dependent. This local high stress can be attributed to the disadvantage of connection between truss and plane continuum. In such case, some measures on the end of truss can be used to reduce the local stress. For example, the designer can introduce the chamfer or rounded corners to reduce stress. This is the reason that we consider the stress in the several layers. In order to determine the local stress, we need local details of connection between truss and plane continuum and carry out continuum analysis. However, the problem of design optimization of the local details is to some extent the same problem as the topics we studied in the entire paper, i.e., the concentrated force diffusion efficiency. Following this idea, it would be expected that the global optimum might be an

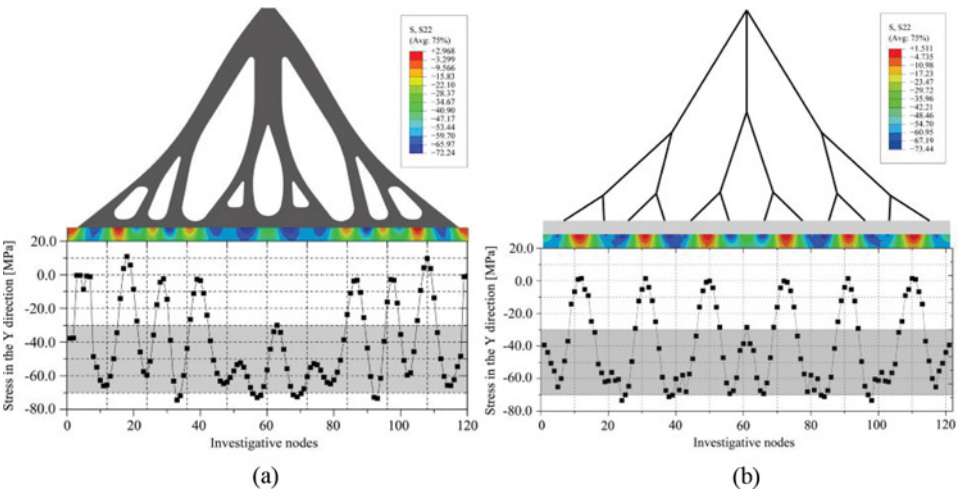


Figure 16 Stress distribution in the Y direction by two strategies: (a) Making holes and (b) Truss-like.

infinite number of branching and hierarchy truss structure, whose geometric features would be infinitely minute. It deserves further study.

6. CONCLUSION

In order to obtain an optimal design of the connection section for concentrated force diffusion, a specialized integrated optimization procedure to design optimization of connection section is preformed. Structural topology optimization with constraints on concentrated force diffusion efficiency is firstly solved. Afterwards, for improving the manufacturability of final design the topology optimization results are interpreted as either truss structure or continuum structure and further optimized by size or shape optimization. Two strategies of interpretation are applied to obtain a further detailed design. The result of making holes strategy shows a more precise identification and interpretation of the result from topology optimization, and more than 70% of stress in the Y direction distributes between 30 and 70 MPa and no obvious regions of high level stress exists. The result of truss-like strategy shows a characteristic of branching and hierarchy structure by interpretation of extraction and recognition. The volume cost of the optimal design of truss-like strategy has a significant reduction, but the design optimization of the local details deserves additional study. The optimal results of two strategies can be applied and accepted by the designer in engineering practice.

FUNDING

The research is supported by the 973 Program (No. 2014CB049000), National Natural Science Foundation of China (11372062, 91216201), LNET Program (LJQ2013005), 111 Project (B14013).

REFERENCES

- Bendsøe, M. P., Sigmund, O. (2003). *Topology Optimization: Theory, Methods, and Applications*. Berlin, Heidelberg.
- Bremicker, M., Chirehdast, M., Kikuchi, N., Papalambros, P. Y. (1991). Integrated topology and shape optimization in structural design. *Mechanics Based Design of Structures and Machines* 19(4):551–587.
- Cheng, G. D., Guo, X. (1997). ϵ -relaxed approach in structural topology optimization. *Structural Optimization* 13(4):258–266.
- Cheng, G. D., Jiang, Z. (1992). Study on topology optimization with stress constraints. *Engineering Optimization* 20(2):129–148.
- Céa, J., Garreau, S., Guillaume, P., Masmoudi, M. (2000). The shape and topological optimizations connection. *Computer Methods in Applied Mechanics and Engineering* 188(4):713–726.
- Deb, K., Pratap, A., Agarwal, S., Meyarivan, T. (2002). A fast and elitist multi-objective genetic algorithm: NSGA-II. *IEEE Trans. On Evolutionary Computation* 6(2):182–197.
- Duysinx, P., Bendsøe, M. P. (1998). Topology optimization of continuum structures with local stress constraints. *International Journal for Numerical Methods in Engineering* 43(8):1453–1478.

- Hsu, M. H., Hsu, Y. L. (2005). Interpreting three-dimensional structural topology optimization results. *Computers & Structures* 83(4–5):327–337.
- Hsu, Y. L., Hsu, M. S., Chen, C. T. (2001). Interpreting results from topology optimization using density contours. *Computers & Structures* 79(10):1049–1058.
- Krog, L., Tucker, A., Rollema, G. (2002). *Application of Topology, Sizing and Shape Optimization Methods to Optimal Design of Aircraft Components*. Airbus UK Ltd., Altair Engineering Ltd.
- Lewinski, T., Rozvany, G. I. N. (2007). Exact analytical solutions for some popular benchmark problems in topology optimization II: three-sided polygonal supports. *Structural and Multidisciplinary Optimization* 33(4–5):337–350.
- Lin, C. Y., Chou, J. N. (1999). A two-stage approach for structural topology optimization. *Advances in Engineering Software* 30(4):261–271.
- Liu, L., Yan, J., Cheng, G. D. (2008). Optimum structure with homogeneous optimum truss-like material. *Computers & Structures* 86(13–14):1417–1425.
- Lógó, J. (2005). New type of optimal topologies by iterative method. *Mechanics Based Design of Structures and Machines* 33(2):149–171.
- Mortenson, M. E. (1985). *Geometric Modeling*. New York: John Wiley & Sons, Inc.
- Olhoff, N., Bendsoe, M. P., Rasmussen, J. (1991). On CAD-integrated structural topology and design optimization. *Computer Methods in Applied Mechanics and Engineering* 89(1–3):259–279.
- Rozvany, G. I. N. (1996). Some shortcomings in Michell's truss theory. *Structural and Multidisciplinary Optimization* 12(4):244–250.
- Rozvany, G. I. N. (2001). Aims, scope, methods, history and unified terminology of computer-aided topology optimization in structural mechanics. *Structural and Multidisciplinary Optimization* 21(2):90–108.
- Rozvany, G. I. N., Gollub, W. (1990). Michell layouts for various combinations of line supports—I. *International Journal of Mechanical Sciences* 32(12):1021–1043.
- Rozvany, G. I. N., Gollub, W., Zhou, M. (1997). Exact Michell layouts for various combinations of line supports—II. *Structural and Multidisciplinary Optimization* 14(2–3):138–149.
- Sigmund, O. (1997). On the design of compliant mechanisms using topology optimization. *Mechanics of Structures and Machines* 25(4):493–524.
- Sigmund, O., Petersson, J. (1998). Numerical instabilities in topology optimization: A survey on procedures dealing with checkerboards, mesh-dependencies and local minima. *Structural and Multidisciplinary Optimization* 16(1):68–75.
- Sokoł, T. (2011). A 99 line code for discretized Michell truss optimization written in Mathematica. *Structural and Multidisciplinary Optimization* 43(2):181–190.
- Sokolowski, J., Zochowski, A. (1999). On the topological derivative in shape optimization. *SIAM Journal on Control and Optimization* 37(4):1251–1272.
- Svanberg, K. (1987). The method of moving asymptotes—a new method for structural optimization. *International Journal for Numerical Methods in Engineering* 24(2):359–373.
- Tang, P. S. (1999). *Integration of Topology and Shape Optimizations for Design of Structural Components*. M.S. Thesis. The University of Oklahoma.
- Tang, P. S., Chang, K. H. (2000). Integration of topology and shape optimization for design of structural components. *Structural and Multidisciplinary Optimization* 22(1):65–82.

- Waller, S. D. (2006). *Mechanics of Novel Compression Structures*. University of Cambridge, Department of Engineering. PHD Thesis.
- Yan, J., Cheng, G. D., Liu, L., Liu, S. T. (2008). Concurrent material and structural optimization of hollow plate with truss-like material. *Structural and Multidisciplinary Optimization* 35(2):153–163.
- Yildiz, A. R., Ozturk, N., Kaya, N., Ozturk, F. (2003). Integrated optimal topology design and shape optimization using neural networks. *Structural and Multidisciplinary Optimization* 25(4):251–260.
- Zhou, K. M., Li, X. (2011). Topology optimization of truss-like continua with three families of members model under stress constraints. *Structural and Multidisciplinary Optimization* 43(4):487–493.